Leaching Chemistry and the Performance of the Mo_6S_8 Cathodes in Rechargeable Mg Batteries

Eli Lancry, Elena Levi, Yossi Gofer, Mikhael Levi, Gregory Salitra, and Doron Aurbach*

Department of Chemistry, Bar-Ilan University, Ramat-Gan, Israel 52900

Received October 2, 2003. Revised Manuscript Received April 29, 2004

The influence of leaching chemistry on the performance of Mo_6S_8 cathodes for rechargeable Mg batteries was studied by XRD, XPS, and electrochemical methods. It is shown that $Cu_2Mo_6S_8$, chemically leached in I_2/AN (acetonitrile) or in HCl/H_2O, is able to accommodate the theoretical amount of Mg^{2+} ions upon the first discharge of the electrode (two Mg atoms per formula unit). In contrast, the process of Mg extraction upon charging the electrode cannot be completed at room temperature, resulting in capacity loss between the first and subsequent cycles. Electrochemical experiments at elevated temperatures reveal that the capacity loss is not related to the leaching process, but results from an intrinsic kinetic problem of the Mg extraction from the $MgMo_6S_8$ phase. Despite the initial capacity loss, the materials leached in I_2/AN or in HCl/H_2O show excellent stability upon long-term cycling, with a specific capacity of 90−100 mA·h/g.

Introduction

Recently, the development of new rechargeable Mg batteries was reported.[1−3] These Mg batteries may be regarded as an analogue to the well-known Li battery because they are based on the same intercalation phenomenon: Li^+ and Mg^{2+} ions from the electrolyte solution are inserted into the host cathode material. However, serious problems have arisen upon the elaboration of the cathode materials for Mg batteries. In fact, a vast variety of compounds, which allow fast and reversible Li insertion, show very poor electrochemical activity in the case of Mg^{2+} ions, despite the basic similarity of the intercalation mechanisms in these systems.[3]

Until now, only one material, Mo_6S_8 with a Chevrel crystal structure, has been suggested as a promising practical candidate for cathodes in Mg batteries.[1−3] Thus, it is very important to study in detail all the stages of the cathode preparation of this unique material. In general, Chevrel phases were intensively studied as superconductors and promising cathodes for Li batteries.[4−6] It was shown that Mo_6S_8, as a thermodynamically unstable material, could be obtained only indirectly by chemical or electrochemical leaching of the more stable, metal-containing Chevrel phases, for example, $Cu_2Mo_6S_8$.[7,8] The phase diagram of the latter material is well-known,[9] while its high-temperature synthesis (1000−1200 °C) from the elements or the sulfides in an evacuated, sealed quartz tube is relatively simple.[10] Note that using $Mg_xMo_6S_8$ obtained by direct high-temperature synthesis should be more attractive, but this material showed poor electrochemical activity. The reason for this phenomenon is still unclear.[11]

According to previous results,[7,8] the removal of Cu from $Cu_2Mo_6S_8$ can be easily performed without damage to the crystal structure. The latter condition seems to be crucial for the cathode's electrochemical performance.[11] However, previous workers did not focus on the leaching process because the development of the new Mg battery technology had not yet been a topical problem.

For instance, in previous works,[8,10] the amount of the residual Cu ions in the Chevrel phase was checked by spectroscopic methods such as atomic absorption or EDAX. These methods are known to be very sensitive, but labor-intensive. Thus, one of our aims was to develop a simpler technique of Cu determination in the leached products, based on XRD measurements. The latter technique allows also an understanding of the mechanism of Cu extraction.

According to Schollhorn et al.,[8] the electrochemical oxidation of $Cu_2Mo_6S_8$ results in complete Cu removal, but it has no technological perspectives since it can be performed only in a separate electrochemical cell due to the detrimental influence of the Cu ions on the

(1) Aurbach, D.; Lu, Z.; Schechter, A.; Gofer, Y.; Gizbar, H.; Turgeman, R.; Cohen, Y.; Moskovich, M.; Levi, E. *Nature* **2000**, *407*, 724.
(2) Aurbach, D.; Gofer, Y.; Lu, Z.; Schechter, A.; Chusid, O.; Gizbar, H.; Cohen, Y.; Ashkenazi, V.; Moskovich, Turgeman, R.; Levi, E. J. *Power Sources* **2001**, *97*, 28.
(3) Aurbach, D.; Weissman, I.; Gofer, Y.; Levi, E. *Chem. Rec.* **2003**, *3*, 61.
(4) Yvon, K. In *Current Topics in Material Science*; Kaldis, E., Ed.; Elsevier: North-Holland, 1979; Vol. 3, pp 53−129.
(5) *Superconductivity in Ternary Compounds I*; Fisher. Ø., Maple, M. B., Eds.; Springer: Berlin, 1982; p 221.
(6) Schollhorn, R. *Angew. Chem., Int. Ed. Engl.* **1980**, *19*, 983.
(7) Chevrel, R.; Sergent, M.; Prigent, J. *Mater. Res. Bull.* **1974**, *9*, 1487.
(8) Schollhorn, R.; Kumpers. M.; Besenhard, J. O. *Mater. Res. Bull.* **1977**, *12*, 781.
(9) Flukiger, R.; Baillif, R. In *Superconductivity in Ternary Compounds I*; Fisher, Ø., Maple, M. B., Eds.; Springer: Berlin, 1982; pp 119−121.
(10) Gocke, E.; Schollhorn, R.; Aselmann, G.; Muller-Warmuth, W. *Inorg. Chem.* **1987**, *26*, 1805.
(11) Levi, E.; Gofer, Y.; Vestfreed, Y.; Lancry, E.; Aurbach, D. *Chem. Mater.* **2002**, *14*, 2767.

10.1021/cm034944+ CCC: $27.50
Published on Web 06/18/2004

surface of Mg anodes in batteries. In contrast, chemical leaching seems to be technologically attractive. Different oxidants, from the very simple, such as HCl or I_2, to the exotic, such as NO_2BF_4, have been mentioned in the literature.[1,7,8,10,12−14] The choice of the oxidant was based on the possible effects to be avoided, such as an insertion of H^+ ions in the Chevrel structure upon leaching in aqueous HCl solutions,[12] or the formation of a small amount of MoS_2 in I_2/acetonitrile (AN) solutions due to excessive oxidation of Mo.[10] Thus, one of the aims of this work was to clarify the sensitivity of the Mo_6S_8 material toward oxidation and to optimize the leaching conditions to avoid undesirable chemical reactions as well as to develop a cheap and technologically feasible method of the cathode material production.

Experimental Section

The Chevrel phase with the intended $Cu_2Mo_6S_8$ composition was synthesized by reaction of the powdered elements mixture in an evacuated, sealed quartz tube. The procedure consisted of four sequential stages: (1) Heating at 450 °C for 24 h; (2) heating at 700 °C for 24 h; (3) heating at 1050 °C for 48 h; (4) cooling down to room temperature at the rate of 120 °C/h.

This synthesis product (1.8 g) was leached under an ambient air atmosphere using three different solutions (20 mL): (i) 6 M HCl in water; (ii) 0.2 M I_2 in acetonitrile (AN); (iii) 0.05 M NO_2BF_4 in AN.

Several days were needed to complete leaching of $Cu_2Mo_6S_8$ in these three solutions. However, it was possible to accelerate the leaching rate in the HCl/H_2O solution by oxygen bubbling. In this case, complete Cu removal required only 7 h. After leaching, the powder was filtered with a fine glass frit, washed with the same solvent, and dried in an oven at 120 °C.

The morphologies of the initial $Cu_2Mo_6S_8$ and leached materials were studied by scanning electron microscopy (SEM) with JSM-6300 JEOL Inc. equipment (Japan).

The electrochemical behavior of the leached materials was studied in standard three-electrode cells using a computerized Arbin Inc. (U.S.A.) multichannel battery tester. Composite cathodes were prepared with 80% active mass, 10% carbon black, and 10% PVdF binder on a stainless steel mesh collector. (The load of the active mass was usually 10 mg/cm^2.) Strips of Mg foil served as counter and reference electrodes. Electrolyte solutions comprising 0.25 M $Mg(AlCl_2BuEt)_2$ in THF (DCC/THF) were used.

XRD studies were performed with a Bruker Inc. (Germany) AXS D8 ADVANCE diffractometer (Cu Kα radiation). Measurements of unstable (air-sensitive) $Mg_xMo_6S_8$ electrodes were carried out in a homemade Al box that was loaded with the active material under a pure argon atmosphere glovebox. The unit cell parameters were refined with WIN-METRIC's program, using Si as an internal standard. The surface chemistry of the leaching products was studied by XPS (Kratos Inc., England, Axis HS spectrometer).

ICP analysis was performed by Aminolab analytical service (Israel).

Results and Discussion

The chemistry of three leaching processes described in the Experimental Section can be presented by the following reactions:

$$Cu_2Mo_6S_8\,(s) + 8HCl\,(aq) + O_2 \rightarrow Mo_6S_8\,(s) + 2H_2O + 2[CuCl_4]^{2-}\,(aq) + 4H^+\,(aq)$$

$$Cu_2Mo_6S_8\,(s) + I_2\,(AN) \rightarrow Mo_6S_8\,(s) + 2CuI\,(AN)$$

$$Cu_2Mo_6S_8\,(s) + 2NO_2BF_4\,(AN) \rightarrow Mo_6S_8\,(s) + 2Cu\,BF_4\,(AN) + 2NO_2\uparrow$$

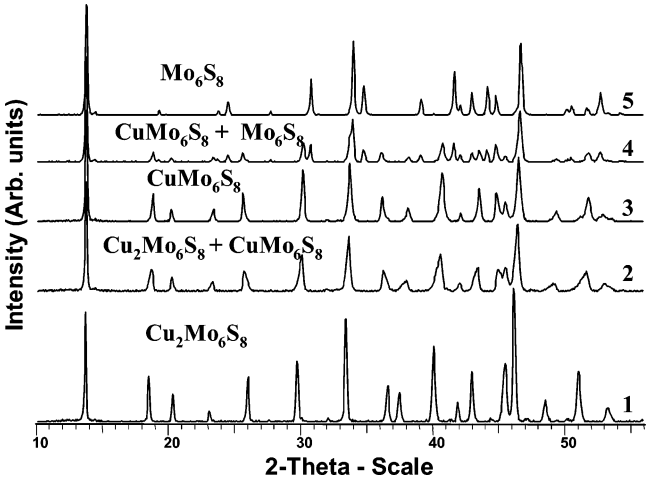

Figure 1. XRD patterns of the Cu_xCP at different stages of leaching: 1, initial synthetic product ($x = 2$); 2, 1 day of leaching ($x \approx 1.5$); 3, 2 days of leaching ($x = 1$); 4, 4 days of leaching ($x \approx 0.5$); 5, 10 days of leaching ($x = 0$).

Thus, the driving force for these reactions is the formation of a stable compound such as CuI, $CuBF_4$, $[CuCl_4]^{2-}$ complex, and NO_2.

As can be concluded from XRD measurement (Figure 1), the initial product of the high-temperature synthesis is almost pure $Cu_2Mo_6S_8$ with only a small amount of MoS_2 impurity (<1%). It is interesting to note that the mechanism of the chemical leaching resembles the electrochemical one.[8] The leaching includes two stages:

$$\text{I. } Cu_2Mo_6S_8 \rightarrow CuMo_6S_8 + Cu^+ + e^-$$

$$\text{II. } CuMo_6S_8 \rightarrow Mo_6S_8 + Cu^+ + e^-$$

Thus, the first stage is the phase transition of $Cu_2Mo_6S_8$ ($a = 9.607(6)$ Å, $c = 10.224(9)$ Å, similar to JCPDS-ICDD, 47-1519) to $CuMo_6S_8$ ($a = 9.459(6)$ Å, $c = 10.375(9)$ Å, similar to JCPDS-ICDD, 34-1379) and the second stage is the phase transition of the latter compound to Mo_6S_8 ($a = 9.200(6)$ Å, $c = 10.880(9)$ Å, similar to JCPDS-ICDD, 27-0319). The phase transitions were clearly deduced by XRD patterns of partially leached products (Figure 1). In fact, the XRD patterns show the decrease of the peaks of one phase and the respective rise of the peaks of the other phase as the leaching process progresses.

Figure 2 presents the relative amount of copper, extracted from $Cu_2Mo_6S_8$ upon leaching in the HCl/H_2O solution as a function of time (no O_2 bubbling). The copper amount was calculated based on the quantitative XRD analysis of progressively leached materials. In fact, the degree of the Cu removal from the material can be established solely by the XRD method with reasonable precision (<6 mass %). As can be seen, removal of the second Cu^+ ion from $Cu_2Mo_6S_8$ is much slower than the first one. Similar kinetics was observed for the other two processes as well. The completion of the leaching process was confirmed by both XRD and ICP analyses.

(12) Guohua, L.; Ikuta, H.; Uchida, T.; Wakihara, M. J. *Power Sources* **1995**, *54*, 519.
(13) Tarascon, J. M.; Waszczak, J. V.; Hull, G. W.; DiSalvo, F. J.; Blitzer, L. D. *Solid State Commun.* **1983**, *47*, 973.
(14) Garcia-Alvarado, F., Tarascon, J. M.; Wilkens, B. J. *Electrochem. Soc.* **1992**, *139*, 3206.

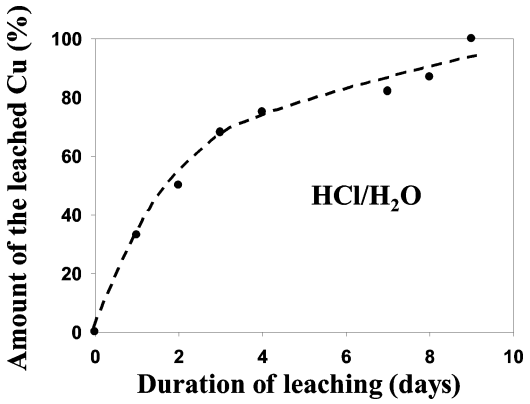

Figure 2. Amount of copper, extracted from the synthetic products upon leaching, vs time (according to the quantitative XRD analysis of the leached materials).

Thus, the amount of Cu (x) in the leached products $Cu_xMo_6S_8$ never exceeded 0.06.

Figure 3 shows SEM micrographs of the leached materials, obtained by the different procedures described above. It can be seen that, in the case of HCl and I_2, the leaching does not change the initial morphology of the crystals and their aggregates, while the process based on NO_2BF_4 as an oxidizer results in pronounced changes of the crystalline shape (compared to $Cu_2Mo_6S_8$) and in the loss of the crystal's integrity.

Figure 4 presents XRD patterns of the Mo_6S_8 products, obtained by three different leaching procedures. In addition to Mo_6S_8, formed by leaching, and the initial MoS_2 impurity, unavoidably present in the synthesis products, the XRD analysis shows also the presence of a small amount of MoO_2. Due to overlapping of the $Cu_2Mo_6S_8$ and MoO_2 diffraction peaks, it was impossible to decide if the latter compound was formed upon oxidation of $Cu_2Mo_6S_8$ in air after synthesis or during leaching. In any event, the MoO_2 impurity appears in the products of all three leaching procedures. It should also be noted that the use of the different oxidizers results in a different intensity of the diffraction peaks. In fact, the integrated intensity of the XRD patterns, calculated as the neat area under the diffraction peaks, was similar for the products leached in HCl/H_2O and I_2/AN, but much smaller for the material leached in NO_2BF_4/AN (only 65%). This decrease in the intensity was not accompanied by any broadening of the diffraction peaks, and thus it could be only explained by partial amorphization of Mo_6S_8. Such interpretation correlates well with the SEM micrographs presented in Figure 3.

Influence of the Leaching Procedure on the Electrode Performance upon Mg Intercalation. To clarify the influence of the various leaching procedures on the electrochemical behavior of the electrode materials, it is important to compare the experimental capacity, related to each stage of the Mg^{2+} insertion/deinsertion into Mo_6S_8, with the theoretical one. To perform such an analysis, we have to know the theoretical electrochemical response of the Mg^{2+} insertion into Mo_6S_8, namely, the stoichiometry of each intercalation phase, the type of the structural changes at different intercalation stages (phase transitions or formation of solid solutions), and the equilibrium potentials corresponding to these stages. The theoretical electrochemical curve of Mg^{2+} insertion into Mo_6S_8 is yet under study and will be published later. At the moment, we can only state that the electrochemical insertion of Mg^{2+} ions into Mo_6S_8 differs from that of Li^+, but is similar to the insertion of other divalent cations, such as Zn^{2+} or Cd^{2+}.[10] Thus, the intercalation of the Mg^{2+} ions occurs in two stages:

$$Mg^{2+} + 2e^- + Mo_6S_8 \rightarrow MgMo_6S_8$$

$$Mg^{2+} + 2e^- + MgMo_6S_8 \rightarrow Mg_2Mo_6S_8$$

Both of these phases can be indexed as rhombohedral (space group $R\bar{3}$), similar to most of the other well-known Chevrel phases.[4,5] The unit cell parameters are as follows: $a = 9.445(6)$ Å and $c = 10.564(9)$ Å for $MgMo_6S_8$ and $a = 9.749(6)$ Å and $c = 10.374(9)$ Å for $Mg_2Mo_6S_8$ (Figure 5).

Figure 6 presents the electrochemical response (chronoamperometry, $E-t$ curves) of the various leached materials. A comparison of the first and the second

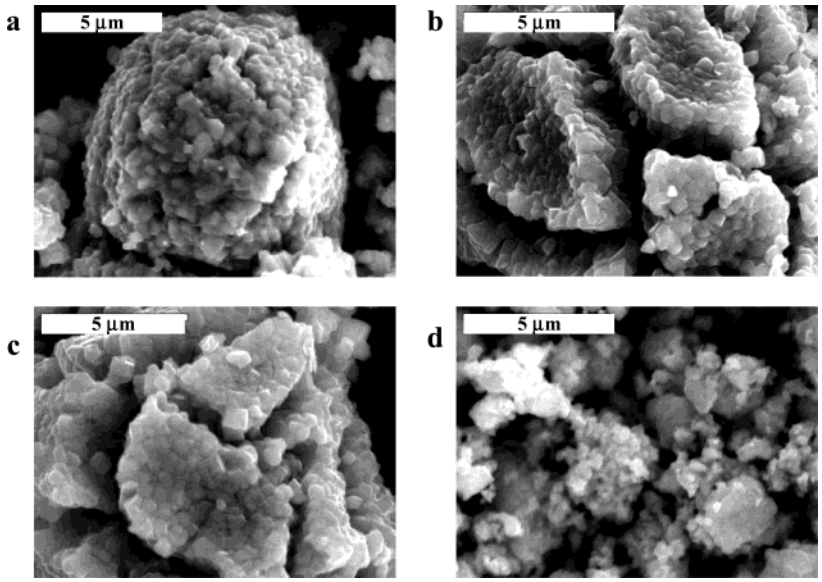

Figure 3. SEM micrographs of the leached materials, obtained as a result of the different reactions: a, initial synthetic product; b, after leaching in HCl/H_2O solution; c, after leaching in I_2/AN solution; d, after leaching in NO_2BF_4/AN solution.

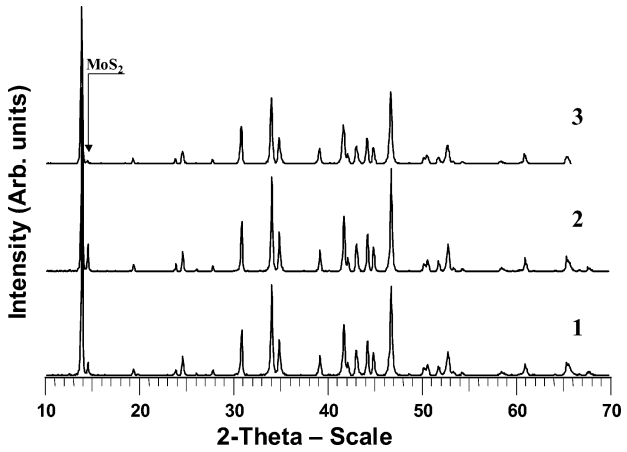

Figure 4. XRD patterns of the leached materials, obtained with different oxidants: 1, HCl/H_2O (9 days of leaching); 2, I_2/AN (8 days of leaching); 3, NO_2BF_4/AN (2 days of leaching).

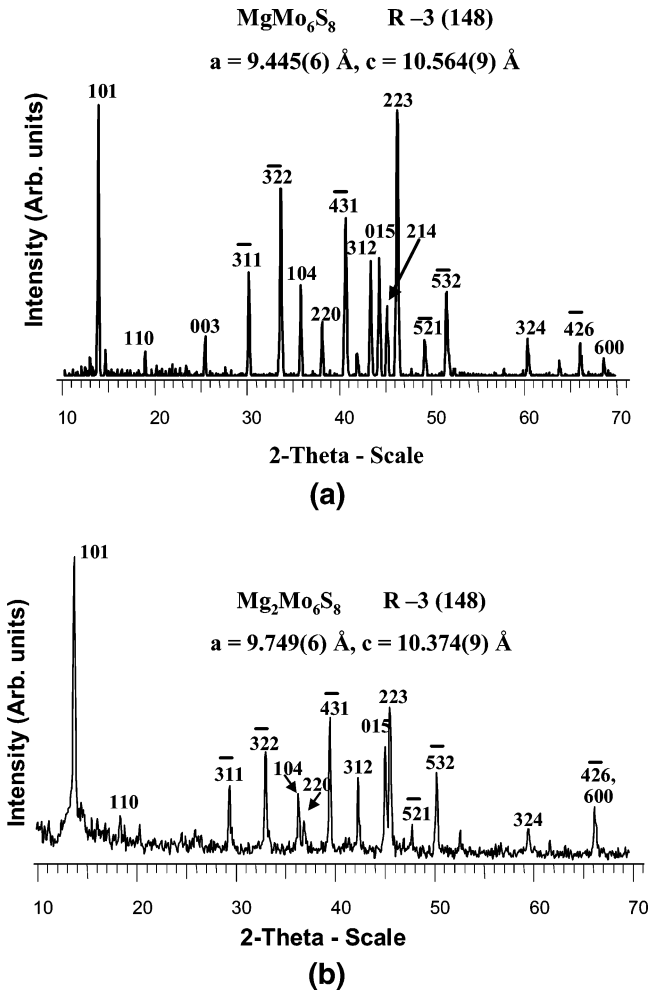

Figure 5. XRD patterns of intercalation compounds: (a) $MgMo_6S_8$; (b) $Mg_2Mo_6S_8$.

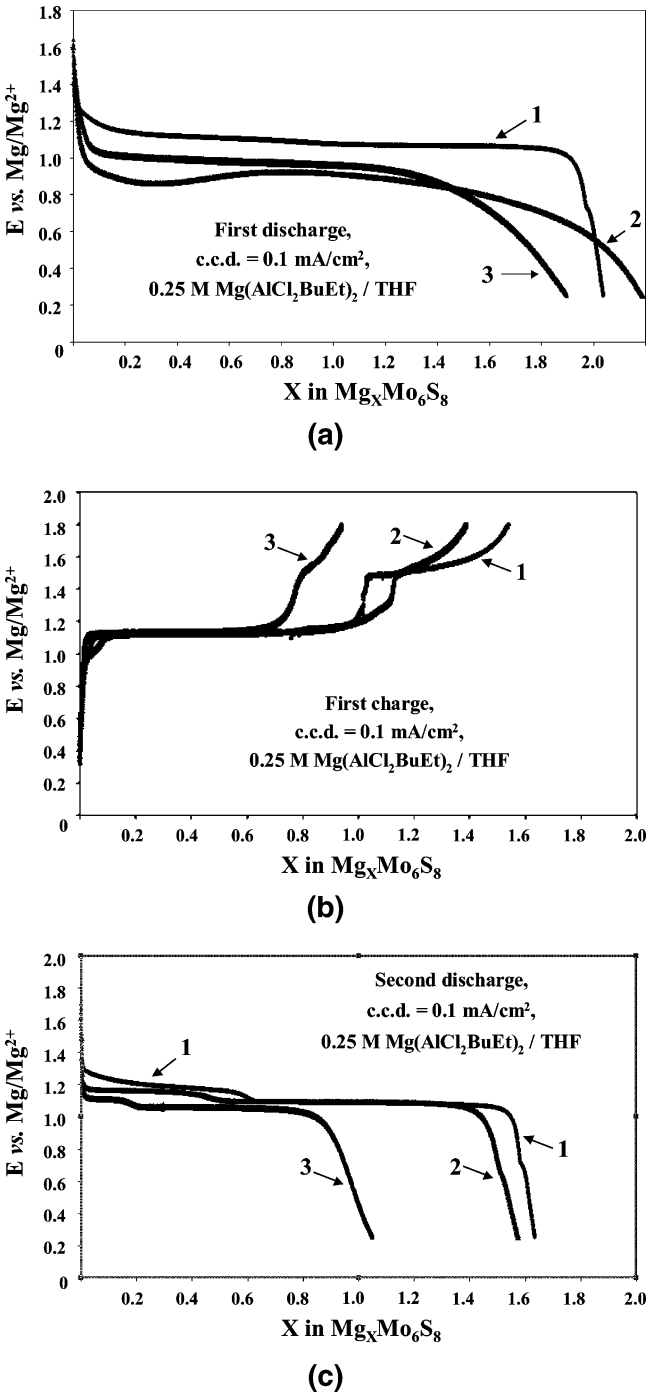

Figure 6. Chronopotentiograms obtained upon galvanostatic polarization of the leached materials: (a) a first discharge, (b) a first charge, (c) second discharge (1, leaching in HCl/H_2O; 2, leaching in I_2/AN; 3, leaching in NO_2BF_4/AN).

discharge curves (a and c, respectively, of Figure 6) shows that the initial Mg^{2+} insertion into Mo_6S_8 is difficult because it needs relatively high over-voltage and takes place at ~1 V instead of 1.2 V. As a result of this over-voltage, the two stages of Mg intercalation take place at a similar or even at an equal potential during the first discharge. Thus, the chronovoltammetric curve upon the first discharge of these materials (i.e., Mg insertion) always demonstrates a single plateau at ~1 V (*v.s.* Mg reference), while two separate plateaus can be clearly distinguished upon the second and the subsequent discharges of the $Mg_xMo_6S_8$ −Mg cells. These features were observed for all the leached materials. However, the over-voltage needed for a first Mg insertion into the material leached in the HCl/H_2O solution is the lowest.

The capacity obtained upon the first discharge of the electrode materials, leached in the HCl/H_2O and the I_2/AN solutions, is usually very close to the theoretical one (122 mA·h/g), while it is a little bit smaller for the material leached in the NO_2BF_4/AN solution. Moreover,

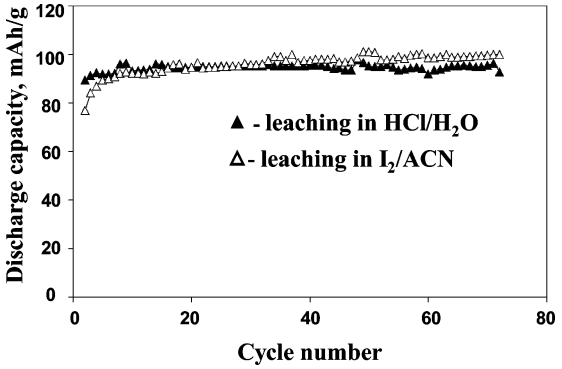

Figure 7. Specific capacity of the leached materials, as cathodes for Mg batteries, upon long-term cycling.

in the latter case one can see a change in the character of the galvanostatic curve, namely, a slow decrease in the potential at the end of discharge, rather than the sharp decrease usually observed at the end of intercalation (i.e., when the active material was leached in HCl/H_2O or I_2/AN solutions). The latter feature shows some difficulty in the intercalation into this material; for example, we could not obtain a fully intercalated $Mg_2Mo_6S_8$ upon discharge down to 0.2 V vs Mg.

The performance of the Mo_6S_8 materials can be assessed more accurately upon the second discharge of the electrodes (Figure 6c). In the case of leaching in HCl/H_2O or I_2/AN solutions, the capacity measured at a second discharge (Mg intercalation) is about 80% of the theoretical one, while it is only 50% with the material leached in NO_2BF_4/AN. In general, a specific capacity, equal to 90−100 mA·h/g, is retained upon prolonged cycling at C/10-C/5 rates for the materials leached in HCl/H_2O or I_2/AN (Figure 7). The same values of the specific capacity obtained with the materials leached under the different conditions (aqueous solution versus nonaqueous solutions) show that the assumptions, mentioned in the literature[10,14] about the possible negative influence of H^+ ions or MoS_2 impurity are incorrect. However, a question arises about the reason for the capacity loss observed for all the leached materials between the first and the subsequent discharges.

First of all, it was important to show that the capacity of the electrodes upon the first discharge (which is close to the theoretical value) is indeed associated only with Mg intercalation, and not with any parasitic reaction. This was verified by XRD analysis of the fully discharged electrodes (see the typical XRD pattern of $Mg_2Mo_6S_8$ in Figure 5). It was found that $Mg_2Mo_6S_8$ is unstable in air. Contact with oxygen leads to its gradual deintercalation. In this case, the XRD pattern shows a mixture of two phases: $Mg_2Mo_6S_8$ and $MgMo_6S_8$. Thus, it is clear from the XRD analysis (when performed properly) that full electrochemical intercalation produces $Mg_2Mo_6S_8$ as the only product, with no side reactions.

The reason for the capacity loss between the first and the subsequent cycles can be understood by analyzing the electrodes' behavior upon oxidation (Mg deintercalation) (Figure 6b). The electrochemical response in Figure 6 also demonstrates a pronounced impact of the leaching chemistry on the electrodes' performance. Similar to intercalation, Mg extraction occurs in two stages. As can be seen in Figure 6b, the first stage of

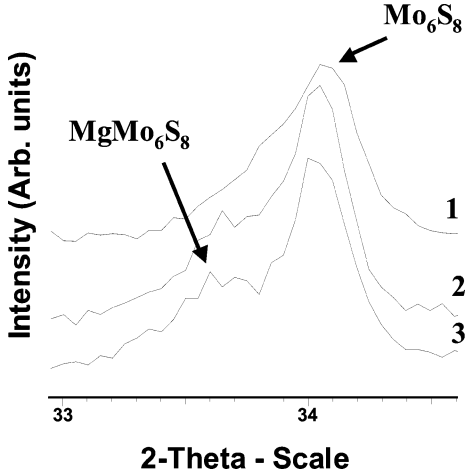

Figure 8. Detailed XRD patterns of the electrode materials in their charged state: 1, leaching in HCl/H_2O; 2, leaching in I_2/AN; 3, leaching in NO_2BF_4/AN.

the Mg deintercalation takes place at the same potential for all leached materials (about 1.1 V), and the capacity related to this stage ($Mg_2Mo_6S_8 \rightarrow MgMo_6S_8$) is close to the theoretical one for the material leached in HCl/H_2O or I_2/AN solution. In contrast, the capacity related to the second deintercalation stage ($MgMo_6S_8 \rightarrow Mo_6S_8$), occurring at 1.5 V, is essentially lower than the theoretical one for all the materials. Hence, the galvanostatic charge of the cells does not result in a full Mg extraction from the Chevrel phase.

Somewhat higher capacity (by 8% more) could be obtained upon deintercalation of these electrodes by polarization at a constant potential of 1.8 V (vs Mg). Thus, a completed Mg deintercalation from these electrodes could not be achieved electrochemically at room temperature. In fact, XRD analysis of the electrodes in the charged state showed that they always contained some amount of $MgMo_6S_8$ (Figure 8). According to these results, it is clear that the capacity loss between the first and the subsequent cycles is caused by the incompleteness of Mg deintercalation. Moreover, the completion of the Mg extraction depends on the leaching chemistry; it is essentially lower for the material leached in NO_2BF_4/AN solution. As a result, one can suggest that the incompleteness of the Mg extraction is connected to the surface films that might form on the active material upon leaching. Such films can hamper the Mg deintercalation due to their low Mg conductivity.

To understand the factors limiting the Mg extraction, the surface chemistry of the leached products was studied by XPS analysis. Figure 9a shows the emission spectra of the materials under study in the wide range of the binding energies. As can be seen, the spectra include oxygen peaks due to the surface oxidation of the material in air. The ratio between the intensities of the oxygen and sulfur peaks is similar for the materials leached in HCl/H_2O and I_2/AN solutions, while it differs essentially for the material treated in the NO_2BF_4/AN solution. According to the intensity of the XPS peaks, the oxygen amount on the surface of the latter material is higher, while the concentration of sulfur is lower, compared to that of the other two materials.

Figure 9b presents the detailed spectra of the Mo(3d) emission for these materials. The samples leached in HCl/H_2O and I_2/AN solutions show two

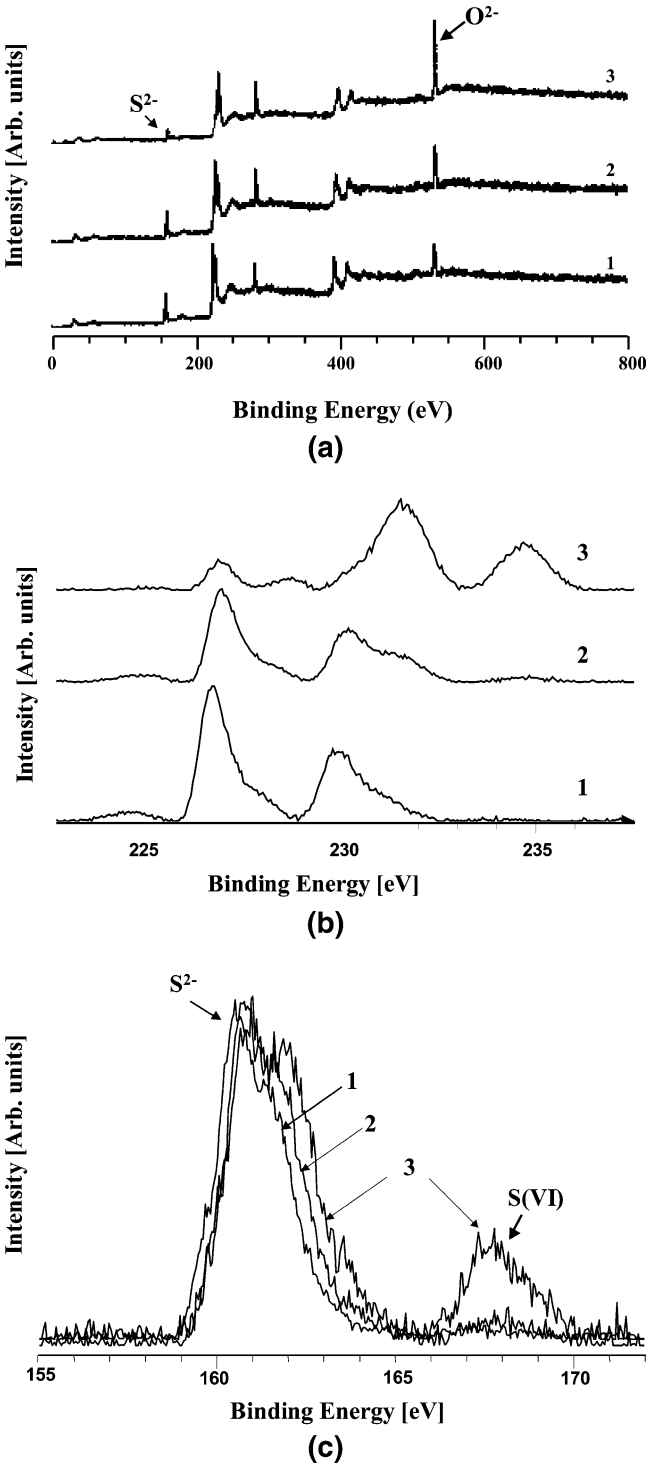

Figure 9. XPS spectra of the leached products: (a) a wide range of binding energy, (b) Mo emission peaks, (c) S emission peaks (1, leaching in HCl/H_2O; 2, leaching in I_2/AN; 3, leaching in NO_2BF_4/AN).

strong Mo(3d) peaks. In the case of the material leached in NO_2BF_4/AN, these peaks are essentially weaker, while two additional strong peaks appear at higher binding energies. It seems difficult to determine the absolute values of the electronic state of the Mo atoms in these samples. However, the shift of the Mo peaks of the latter material to the higher binding energy unambiguously proves that its surface is at a higher oxidation state compared to those of the other two materials. A similar conclusion arises from the analysis of the sulfur peaks (Figure 9c): For the materials leached in HCl/H_2O and I_2/AN, the spectra present only peaks related to S^{2-}, while an additional peak, caused by the presence of S(VI), appears in the spectra of the material leached in NO_2BF_4/AN.

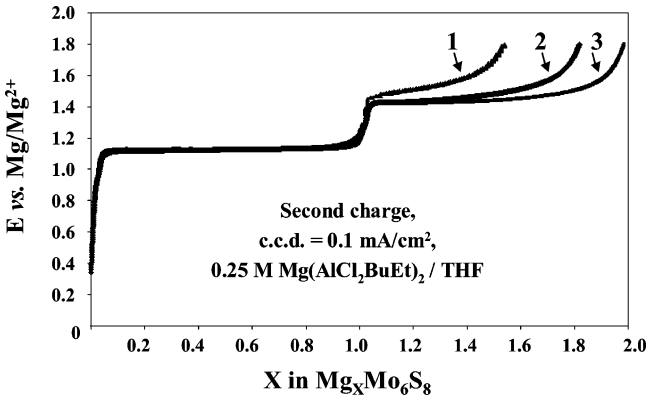

Figure 10. Chronopotentiograms ($V-t$ curves in galvanostatic experiments) of the material leached in HCl/H_2O upon charge at different temperatures: 1, 30 °C; 2, 45 °C; 3, 60 °C.

Thus, the XPS analysis shows that the oxidation state of Mo and S atoms on the surface of the materials, leached in HCl/H_2O and I_2/AN, is very similar, while it is essentially different for the material leached in such a strong oxidizer as NO_2BF_4/AN. In the latter case, the concentration of surface oxygen is effectively higher, and the formation of Mo sulfate seems to be evident. Thus, oxidation of the material upon leaching can be responsible for some limitation of the cathode activity in the case of NO_2BF_4/AN, but it seems insignificant in the case of HCl/H_2O and I_2/AN.

It is reasonable to suggest that this limitation results from some intrinsic kinetic problem of the cation deintercalation in these materials. In fact, a similar phenomenon of incomplete deintercalation has been reported for Na^+ extraction from $Na_XMo_6S_8$.[15] It is well-known that kinetics of most chemical/electrochemical processes can be pronouncedly improved by increasing the temperature. Thus, to verify the influence of the Mg^{2+} ions' kinetics on the Mg extraction, the cycling was performed at different temperatures. As can be seen in Figure 10, the temperature increase results in a drastic increase of the charge capacity, and a full Mg extraction (up to the theoretical capacity of 122 mA·h/g) takes place at 60 °C.

Hence, the capacity loss between the first and the subsequent cycles results from an intrinsic kinetic problem of the Mg extraction from the Chevrel phase and is not due to any side reactions (surface deactivation by oxidation, interactions with solution species etc.). Moreover, this initial capacity loss at room temperature does not at all affect the excellent stability of the leached materials upon long-time cycling (Figure 7).

It is interesting to note that sometimes an additional potential plateau at 0.8 V can be observed in the galvanostatic curves of the leached materials. It can be suggested that this plateau appears as a result of an uncompleted leaching, due to the presence of Cu^+ ions in the Chevrel phase. To verify this suggestion, samples

(15) Tarascon, J. M.; Hull, G. W.; Marsh, P.; Ter Haar J. *Solid State Chem.* **1987**, *66*, 204.

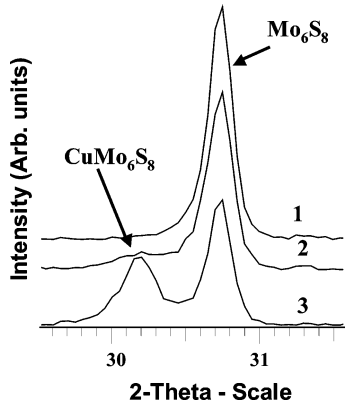

Figure 11. Detailed XRD patterns of the leached product, $Cu_XMo_6S_8$, with different amounts of residual Cu: 1, $x \approx 0$; 2, $x \approx 0.15$; 3, $x \approx 0.3$.

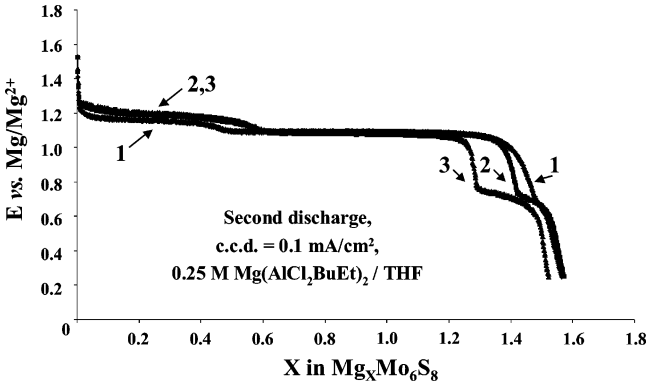

Figure 12. Chronopotentiograms ($V-t$ curves in galvanostatic experiments) of the leached (HCl/H_2O solution) product, Cu_X-Mo_6S_8, with different amounts of residual Cu: 1, $x \approx 0$; 2, $x \approx 0.15$; 3, $x \approx 0.3$.

with different residual Cu amounts were prepared by controlled leaching. Figure 11 shows the XRD patterns of these samples that differ by the relative amount of two phases: $CuMo_6S_8$ and Mo_6S_8. As can be seen in Figure 12, the charge associated with the plateau at 0.8 V correlates well with the amount of Cu-containing Chevrel phase in the leached materials.

On the basis of these results, we suggest that this plateau relates to the Mg intercalation into $CuMo_6S_8$. In fact, it was shown that the presence of Cu in the Chevrel crystal structure does not disturb insertion of Li^+ ions.[16] In the case of Li, intercalation results also in the removal of Cu^+ ions from the Chevrel crystal structure with no deterioration in the performance of the cathode material.[12,17] More careful work (beyond the scope of this paper) is needed to clarify the mechanism of Mg intercalation into Cu-containing Chevrel phases.

Conclusion

The combination of XRD, XPS, and electrochemical methods was used to study the chemistry of Cu extraction from $Cu_2Mo_6S_8$, as well as its influence on the electrochemical performance of the leached products, used as an active mass in the cathodes for rechargeable Mg batteries. Similar to the electrochemical process of Cu extraction, the chemical leaching occurs in two stages: The first stage is the phase transition of Cu_2-Mo_6S_8 to $CuMo_6S_8$, while the second stage is the phase transition of $CuMo_6S_8$ to Mo_6S_8. These stages have completely different kinetics: The first Cu^+ ion from the initial $Cu_2Mo_6S_8$ leaches very easily, while the extraction of the second one happens much slower. It was shown that $Cu_2Mo_6S_8$, chemically leached in I_2/AN or in HCl/H_2O, is able to accommodate a theoretical amount of Mg^{2+} ions upon the first discharge (cathodic polarization) of the electrode at a current density of 0.1 mA/cm^2 (two Mg atoms per formula unit, Mo_6S_8). In contrast, consequent electrochemical extraction of Mg from these electrodes cannot be completed at room temperature, resulting in capacity loss between the first and the subsequent cycles. Electrochemical experiments at elevated temperatures reveal that the capacity loss is not related to the leaching process or any side reactions, but result from an intrinsic kinetic problem in the Mg extraction from the Chevrel phase. Despite the initial capacity loss, the materials leached in I_2/AN or in HCl/H_2O solutions show an excellent stability upon long-term cycling, with a specific capacity of 90−100 mA·h/g at C/10−C/5 rates.

Acknowledgment. Partial support for this work was obtained by the ISF, Israel Scientific Foundation, and ATU Ltd/Israel.

Supporting Information Available: XRD patterns of the Chevrel active material in the discharge state (PDF). This material is available free of charge via the Internet at http://pubs.acs.org.

CM034944+

(16) McKinnon, W. R.; Dahn, J. R. *Solid State Commun.* **1984**, *52*, 245.

(17) Takeda, Y.; Kanno, R.; Noda, M.; Yamamoto, O. *Mater. Res. Bull.* **1985**, *20*, 71.